# Multichannel Surface Plasmon Resonance Imaging and Analysis of Micropatterned Self-Assembled Monolayers and Protein Affinity Interactions

**ARTICLE** *in* LANGMUIR · FEBRUARY 2005

Impact Factor: 4.46 · DOI: 10.1021/la0486382 · Source: PubMed



**4 AUTHORS**, INCLUDING:

Hyeon-Bong Pyo
Electronics and Telecommunications Resear…
**35** PUBLICATIONS **313** CITATIONS
SEE PROFILE

Yong-Beom Shin
Korea Research Institute of Bioscience and B…
**74** PUBLICATIONS **1,300** CITATIONS
SEE PROFILE

Hyun C Yoon
Ajou University / Korea
**87** PUBLICATIONS **1,852** CITATIONS
SEE PROFILE

# Multichannel Surface Plasmon Resonance Imaging and Analysis of Micropatterned Self-Assembled Monolayers and Protein Affinity Interactions

Hyeon-Bong Pyo,*,† Yong-Beom Shin,‡ Min-Gon Kim,‡ and Hyun C. Yoon*,§

*Basic Research Laboratory, Electronics and Telecommunications Research Institute, Daejon 305350, Korea, Laboratory of Integrative Biotechnology, Korea Research Institute of Bioscience and Biotechnology, Daejon 305333, Korea, and Department of Biotechnology, Ajou University, Suwon 442749, Korea*

*Received June 2, 2004. In Final Form: October 21, 2004*

Multichannel images of 11-mercaptoundecanoic acid and 11-mercapto-1-undecanol self-assembled monolayers together with a biospecific interferon-$\gamma$ (IFN-$\gamma$)/anti-IFN-$\gamma$ antibody immunoaffinity interaction were observed by the two-dimensional surface plasmon resonance (2D-SPR) imaging system. With the fabricated 2D-SPR imaging system, adopting a white light source in combination with a narrow band-pass filter, sharp images were resolved, minimizing the diffraction patterns on the resulting images. Micropatterning of self-assembled monolayers was acheived by exploiting the UV photolysis of thiol bonding, instead of conventional photolithography. The line profile calibration of the image contrast with ellipsometric analysis enabled us to discriminate the change in monolayer thickness within a sub-nanometer scale. For the protein interactions on the surface, the biospecific affinity recognition reaction of IFN-$\gamma$ antigen with surface-immobilized antibody was analyzed. Through the signal amplification strategy based on the enzyme-catalyzed precipitation reaction in a sandwich-type immunoassay, biospecific antigen binding was found detectable down to a concentration of 1 ng/mL.

## 1. Introduction and Theory

Surface plasmon polaritons (SPPs) or simply surface plasmons (SPs) are longitudinal, collective oscillations of electrons on the metal−dielectric interface.[1−3] Because SP waves are inherently longitudinal, they can be coupled only with the transverse magnetic (TM) mode of electromagnetic waves. Contrary to volume plasmons, which are unable to be excited by light, surface plasmons can be coupled with incident light by using a prism coupler or by employing corrugated metal surfaces (metal gratings) to enhance the momentum of incident light.[2] Recently, methods of making protrusions or apertures in a sub-wavelength scale have been developed and attracted a fair amount of attention, mainly from their potential applicability to many research fields, ranging from nanoscaled photonics devices (e.g., filters, switches, and data storage media)[4−6] to chemosensors and biosensors (e.g., surface-enhanced Raman scattering/spectroscopy).[7−10]

While SPs propagate along the metal−dielectric interface until their energy is dissipated in the metal, they are nonradiative and bound in the normal direction across the metal−dielectric interface. Therefore, the SP field is evanescent. The electric field intensity that is normal to the interface decays exponentially, reflecting the limited sensitivity of the SP-based sensor system. However, if the optical properties of the dielectric, including refractive index, thickness, and so forth, have been changed, one can "tune" the parameters such as the incident angle and/or wavelength of light to retain the desired SP coupling condition.[2,3]

To obtain more insight into the characteristics of SPs, analysis of the energy−momentum relationship of the system, the dispersion relation of SPs, is needed. On the basis of the Maxwell equations with proper boundary conditions, the dispersion relation of SPs can be found as

$$k_{sp} = \frac{\omega}{c}\sqrt{\frac{\epsilon_1(\omega)\epsilon_2}{\epsilon_1(\omega) + \epsilon_2}} \qquad (1)$$

where $k_{sp}$ is the wavevector of SPs and $\epsilon_1(\omega)$ and $\epsilon_2$ are complex dielectric functions of the metal and dielectric, respectively. Because the wavevector $k_{sp}$ is larger than that of light ($\omega/c$) in vacuo, an additional amount of $k$ needs to be added on the net wavevector of light ($\omega/c$). One of the most frequently employed methods is attenuated total reflection (ATR) using a prism coupler.[11,12] Because the effective momentum of light when it goes through a transparent dielectric medium holds the relation $\epsilon_0^{0.5}(\omega/$

* Authors to whom correspondence should be addressed. E-mail: pyo@etri.re.kr (H.-B.P.); hcyoon@ajou.ac.kr (H.C.Y.).
† Electronics and Telecommunications Research Institute.
‡ Korea Research Institute of Bioscience and Biotechnology.
§ Ajou University.

(1) Barnes, W. L.; Dereux, A.; Ebbesen, T. W. *Nature* **2003**, *424*, 824−830.
(2) Raether, H. *Surface Plasmons on Smooth and Rough Surfaces and on Gratings*; Springer: Berlin, 1988.
(3) Agranovich, V. M.; Mills, D. H. *Surface Plasmons: Electromagnetic Waves at Surfaces and Interfaces*; North-Holland: Amsterdam, The Netherlands, 1982.
(4) Ebbesen, T. W.; Lezec, H. J.; Ghaemi, H. F.; Thio, T.; Wolff, P. A. *Nature* **1998**, *391*, 667−669.
(5) Barnes, W. L.; Murray, W. A.; Dintinger, J.; Devaux, E.; Ebbesen, T. W. *Phys. Rev. Lett.* **2004**, *92*, 107401.1−107401.4.
(6) Schroter, U.; Heitmann, D. *Phys. Rev. B* **1999**, *60*, 4992−4999.
(7) Ruperez, A.; Laserna, J. J. Surface enhanced Raman spectroscopy. In *Modern Techniques in Raman Spectroscopy*; Laserna, J. J., Ed.; John Wiley & Sons: Chichester, U.K., 1996.
(8) Cotton, T. M. The application of surface-enhanced Raman scattering to biochemical systems. In *Spectroscopy of Surfaces*; Clark, R. J. H., Hester, R. E., Eds.; John Wiley & Sons: NewYork, 1988.
(9) Jiang, C.; Markutsya, S.; Tsukruk, V. V. *Langmuir* **2004**, *20*, 882−890.
(10) Yonzon, C. R.; Haynes, C. L.; Zhang, X.; Walsh, J. T., Jr.; Van Duyne, R. P. *Anal. Chem.* **2004**, *76*, 78−85.
(11) Dawson, P.; Puygranier, B. A. F. *Phys. Rev. B* **2001**, *63*, 205410.1−205410.9.
(12) Bradshaw, J. T.; Mendes, S. B.; Saavedra, S. S. *Anal. Chem.* **2002**, *74*, 1751−1759.

10.1021/la0486382 CCC: $30.25 
Published on Web 12/08/2004

$c) = n_0(\omega/c)$ ($\epsilon_0$, dielectric function; $n_0$, refractive index), the coupling condition of the SPs with light at the same energy is

$$k_x = \frac{\omega}{c}\sqrt{\epsilon_0}\sin\theta_0 = \frac{\omega}{c}n_0\sin\theta_0 = k_{sp} \qquad (2)$$

and

$$n_0\sin\theta_0 = \sqrt{\frac{\epsilon_1(\omega)\epsilon_2}{\epsilon_1(\omega)+\epsilon_2}} \qquad (3)$$

We considered only the $x$-component ($k_x$) along the interface, where $\theta_0$ is the incident angle of light, since other components of the photon wave vector do not contribute to the SP excitation.

From eq 3, we easily see that for constant $n_0$, if the $\epsilon_2$ value of the dielectric material (e.g., sample analyte) has been changed, one can retain the SP coupling condition by varying either the incident angle ($\theta_0$) or the dielectric function of the metal ($\epsilon_1(\omega)$), which is dependent on the energy (wavelength) of light. These two modes of variation, called angle and wavelength interrogation, determine the sensitivity and resolution of the SPR-based sensor. From experiments, the SP resonance data are obtained by measuring reflectivity as a function of either the incident angle or the wavelength, and reflectivity can be calculated by the n-phase Fresnel equation.[13]

As a typical example, the reflectivity of the four-layered system BK7/Cr (2 nm)/Au (45 nm)/X, where X is either air or water as an analyte sample, was calculated and plotted as a function of the angle and wavelength of incident light (Figure 1). BK7 is a glass material for the prism coupler in this layer configuration. From Figure 1 and its contour plot (Figure 2), the SP resonance was registered at $\theta_0 = 42.4°$ at a wavelength of 830 nm for air, while a resonance angle shift to a higher angle of $\theta_0 = 65.2°$ was observed for water (refractive index 1.33) at the same wavelength. A more important observation here was that the width of the resonance dip was dependent on the wavelength of light, so one must take care in selecting an optimal wavelength of light for the best possible thickness resolution of the fabricated system. Moreover, above an energy of ~520 nm (at shorter wavelengths), the photons do not transfer their energies to the plasmon mode of electrons. Rather, they transfer their energies to the individual electrons for excitation (interband transition), resulting in the disappearance of the SP resonance. Thus, we carried out most of our experiments with lasers of either 633 or 830 nm in wavelength or with a quartz tungsten−halogen (QTH) lamp as a white light source.

On the basis of the developed theory, recent years have witnessed the appearance of several interesting technologies extended from SPR spectroscopy,[14,15] including miniaturized and integrated SPR sensor chips (Spreeta),[16−18] hybrid systems with mass spectroscopy (BIA/MS) or electrochemistry,[19,20] and SPR imaging systems.[21−26]

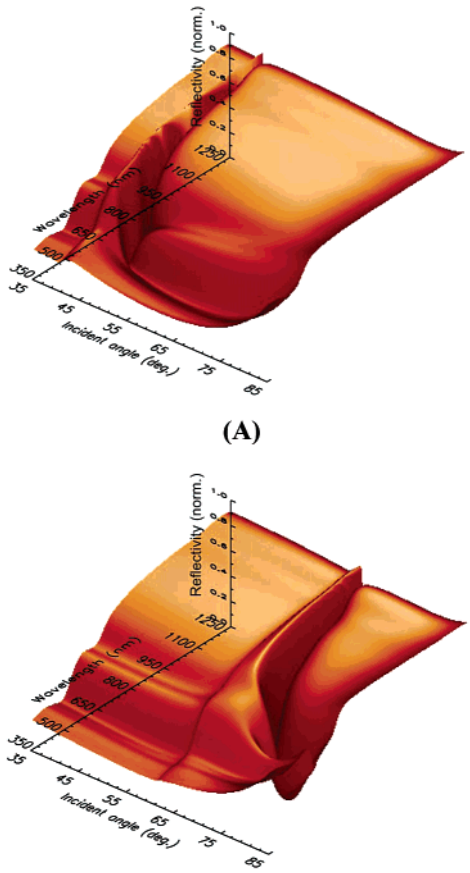


**Figure 1.** Reflectivity ($z$-axis) of BK7/Cr (2 nm)/Au (45 nm)/X (sample) represented by the resonance absorption dip as a function of incident angle and wavelength of light calculated using the n-phase Fresnel equation: (A) X is air ($n_D = 1.0$); (B) X is water ($n_D = 1.33$) (with the same SPR chip configuration).

In this paper, we describe the development of a two-dimensional surface plasmon resonance (2D-SPR) imaging system based on the above theory and calculations as well as its application to surface analysis. With the fabricated 2D-SPR imaging system, multichannel images of micropatterned thiol self-assembled monolayers (SAMs) were collected and analyzed. The registered film thickness data from micropatterned SAMs were compared with the ellipsometric data to calibrate the 2D-SPR imaging system. In addition, to evaluate the possibility of using the 2D-SPR imaging system as a protein chip platform, biospecific antigen/antibody affinity interactions were also examined. Details are reported herein.

## 2. Experimental Section

**2.1. Materials.** 11-Mercaptoundecanol and 11-mercaptoundecanoic acid were purchased from Aldrich and used as received. *N*-hydroxysuccinimide (NHS), 1-ethyl-3-(3-dimethylaminopro-

(13) Hansen, W. N. *J. Opt. Soc. Am.* **1968**, *58*, 380−390.
(14) Jonsson, U.; Fagerstam, L.; Ivarsson, B.; Johnsson, B.; Karlsson, R.; Lundh, K.; Lofas, S.; Persson, B.; Roos, H.; Ronnberg, I.; Sjolander, S.; Stenberg, E.; Stahlberg, R.; Urbaniczky, C.; Ostlin, H.; Malmqvist, M. *BioTechniques* **1991**, *11*, 620−627.
(15) Malmqvist, M. *Nature* **1993**, *361*, 186−187.
(16) Elkind, J. L.; Stimpson, D. I.; Stong, A. A.; Bartholomew, D. U.; Melendez, J. L. *Sens. Actuators, B* **1999**, *54*, 182−190.
(17) Whelan, R. J.; Wohland, T.; Neumann, L.; Huang, B.; Kobilka, B. K.; Zare, R. N. *Anal. Chem.* **2002**, *74*, 4570−4576.
(18) Hong, M. Y.; Yoon, H. C.; Kim, H. S. *Langmuir* **2003**, *19*, 416−421.
(19) Nedelkov, D.; Nelson, R. W. *Biosens. Bioelectron.* **2001**, *16*, 1071−1078.
(20) Raitman, O. A.; Katz, E.; Bückmann, A. F.; Willner, I. *J. Am. Chem. Soc.* **2002**, *124*, 6487−6496.
(21) Rothenhhäusler, B.; Knoll, W. *Nature* **1988**, *332*, 615−617.
(22) Yeatman, E.; Ash, E. *Electron. Lett.* **1987**, *23*, 1091−1092.
(23) Nelson, B. P.; Grimsrud, T. E.; Liles, M. R.; Goodman, R. M.; Corn, R. M. *Anal. Chem.* **2001**, *73*, 1−7.
(24) Smith, E. A.; Erickson, M. G.; Ulijasz, A. T.; Weisblum, B.; Corn, R. M. *Langmuir* **2003**, *19*, 1486−1492.
(25) Fu, E.; Foley, J.; Yager, P. *Rev. Sci. Instrum.* **2003**, *74*, 3182−3184.
(26) Steiner, G. *Anal. Bioanal. Chem.* **2004**, *379*, 328−331.

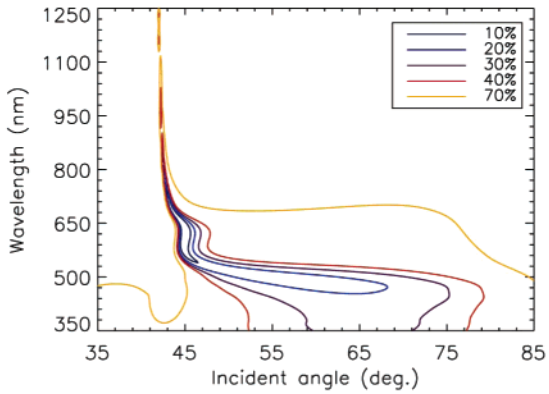


**(A)**

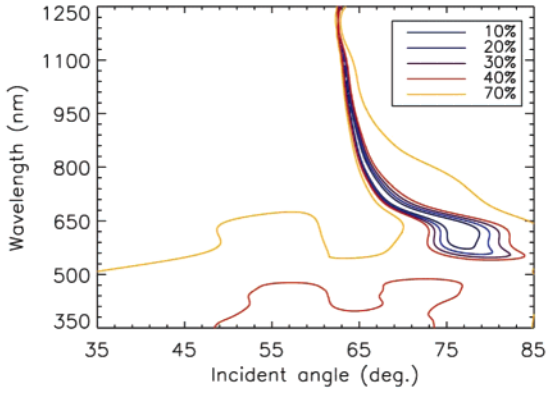


**(B)**

**Figure 2.** Contour plots of Figure 1. The width of the SP resonance dip is smaller for longer wavelengths at a fixed angle. If the refractive index (RI) of the dielectric becomes larger, the SP resonance angle and wavelength also become larger and longer. Therefore, when monochromatic light is used, it is better to take a near-infrared (NIR) light source than a visible light source for better angle resolution. (A) For air: for $\lambda = 633$ nm, the SP resonance minimum occurs at an incident angle of $\theta = 44.9°$, while, for $\lambda = 830$ nm, it occurs at $\theta = 42.4°$. (B) For water: for $\lambda = 633$ nm, the SP resonance minimum occurs at an incident angle of $\theta = 76.4°$, while, for $\lambda = 830$ nm, it occurs at $\theta = 65.2°$.

pyl)carbodiimide hydrochloride (EDAC), and 4-chloro-1-naphthol (4-CN) were purchased from Sigma. Matched pair antibodies for interferon-$\gamma$ (IFN-$\gamma$), anti-interferon-$\gamma$ (anti-IFN-$\gamma$) capture antibody, and biotinylated anti-IFN-$\gamma$ detection antibody were obtained from Santa Cruz Biotechnology. Interferon-$\gamma$ as a target antigen, bovine serum albumin (BSA), horseradish peroxidase (HRP)-labeled avidin (avidin−HRP), and anti-interleukin-5 (anti-IL-5) antibody were obtained from Sigma and used without further purification. All other materials used were of the highest quality available and purchased from regular sources.

**2.2. Sample Preparation and Surface Patterning.** Patterned SAMs or proteins on a gold-coated chip surface were prepared as follows. First, a 2 nm chromium adhesion layer and plasmon-supporting gold layer of a 45 nm thickness were deposited successively on a 22 mm × 22 mm cover glass by an electron beam evaporator. The thickness of each layer was chosen for optimal SPR characteristics on the basis of theoretical calculations (vide supra). Prior to vacuum evaporation, cover glasses were cleaned in Piranha solution (concentrated $H_2SO_4$/30% $H_2O_2$, 4:1 v/v) and successively rinsed with acetone and deionized (DI) water. *CAUTION: Piranha solution reacts violently with most organic materials and must be handled with extreme care.* The evaporation was performed under $1.6 \times 10^{-6}$ Torr with a deposition rate of ~0.5 nm/s. While the preparation of the gold-coated sensor surface was essentially the same for patterned SAMs and proteins, the patterning processes were different. For SAM patterning, freshly evaporated, gold-coated

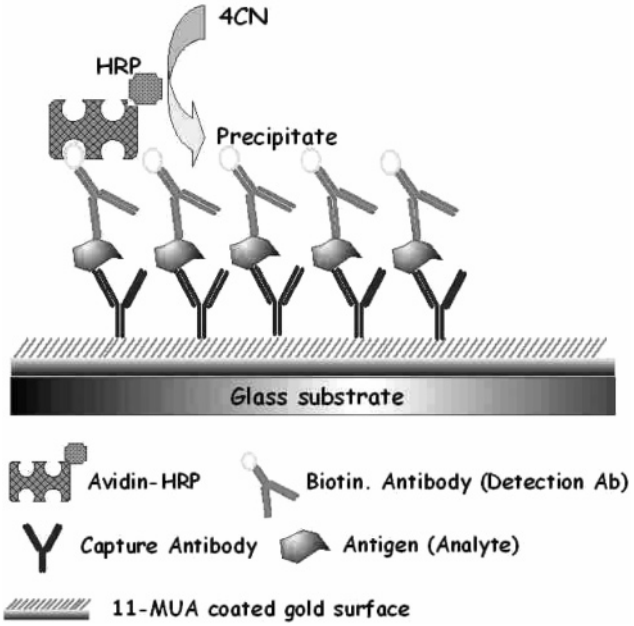


**Figure 3.** Schematic illustration of the sandwich-type immunoassay employed in this study. The resulting chip surface configuration having avidin−HRP/biotinylated anti-IFN-$\gamma$/IFN-$\gamma$ antigen/anti-IFN-$\gamma$ capture antibody/SAM association laminate was depicted with the biocatalyzed signal amplification step via immunoprecipitation. For simplicity, the dimensions of the components are not drawn to scale.

cover glasses were immersed in either 10 mM 11-mercaptoundecanol or 11-mercaptoundecanoic acid in ethanol for 24 h at 25 °C.

**2.2.1. Patterning Process for the 11-Mercaptoundecanol SAM on the Gold Surface.** After formation of the 11-mercaptoundecanol SAM on gold, a photoresist (AZ5214E, Hoechst) was spin-coated and baked on a hot plate with a thickness of ~1 $\mu$m. A chrome photomask micropatterned with circle arrays (diameter 300 $\mu$m) was fabricated and placed on the SAM-formed surface. Then, the surface was exposed with a 365 nm UV light using a mask aligner and developed by a developer. The exposed SAM area was photooxidized from alkynethiolates to alkynesulfonates ($SO^{3-}$) by an UV illumination (150 W xenon lamp, 5 h) and washed by ethanol.[27,28] Residual photoresist was then removed by acetone, and the whole sensor surface was rinsed thoroughly by ethanol.

**2.2.2. Direct Patterning of the 11-Mercaptoundecanoic Acid SAM on the Gold Surface.** For the patterning of the 11-mercaptoundecanoic acid SAM, we applied a more simplified method of alkanethiolate bond photooxidation (photolysis). We fabricated a metal shadow mask in which arrays of circular holes (diameter 300 $\mu$m) are regularly spaced. The shadow mask was then placed in close proximity on the SAM-coated sensor surface. The sensor chip with the shadow mask was clamped together and exposed to a 1000 W Hg(Xe) lamp for 5 h, washed with ethanol, and dried with nitrogen gas. After photooxidation by UV light, only the exposed parts of the SAM were removed, forming a micropattern of holes array. While the photooxidation processes in both methods were essentially similar, the proper condition of the intensity of UV light was differently chosen.

**2.2.3. Biochip Sample Preparation for Biospecific Protein Interactions.** A schematic illustration of the immunoassay procedure employed in the present study is shown in Figure 3. The 11-mercaptoundecanoic acid SAM on the gold surface was activated as a hydroxysuccinimidyl ester by incubating it with a mixture of NHS (0.05 M) and 1-ethyl-3-(3-dimethylaminopropyl)carbodiimide hydrochloride (EDAC, 0.2 M) in DI water. The activated chip was then washed with DI water and spun on a

(27) Huang, J.; Hemminger, J. C. *J. Am. Chem. Soc.* **1993**, *115*, 3342−3343.
(28) Huang, J.; Dahlgren, D. A.; Hemminger, J. C. *Langmuir* **1994**, *10*, 626−628.

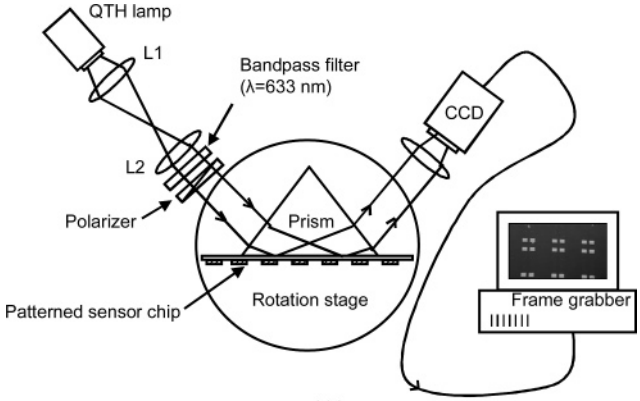


(A)

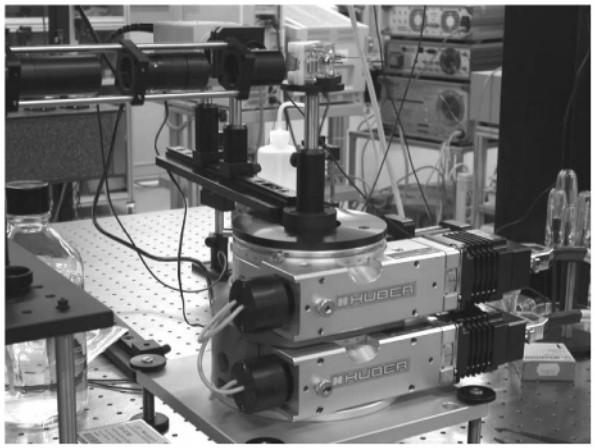

(B)

**Figure 4.** (A) Schematic illustration of the 2D-SPR imaging system. The patterned layer on the gold-coated cover glass was optically coupled with a prism coupler (BK7) and located on the top of a $\theta-2\theta$ goniometer. L1 and L2 are focusing and collimating lenses, and QTH stands for quartz tungsten−halogen lamp. (B) An in-house-built 2D-SPR imaging system for the experiments.

spinner at 2000 rpm for 5 min for drying. Capture antibodies, anti-IFN-$\gamma$ antibody, and anti-IL-5 antibody (100 $\mu$g/mL in 10 mM acetate buffer at pH 5.4) together with BSA (1 mg/mL in phosphate-buffered saline (PBS)) as a control sample were regularly spotted (diameter 300 $\mu$m) side by side using microarraying equipment on the NHS-activated chip surface. The patterned and protein-immobilized chip was then incubated with a BSA solution (1%) for blocking of the unreacted sites and in turn with IFN-$\gamma$ antigen solution containing 1 mg/mL BSA. After thorough washing with PBS to remove nonspecifically bound IFN-$\gamma$, the chip was then incubated with the mixture of biotinylated detection antibody of IFN-$\gamma$ and avidin−HRP (20 $\mu$g/mL each). Finally, for the immunoprecipitation reaction for signaling, the reaction solution containing $H_2O_2$ (1 mM) and 4-CN (1 mM) was added to the chip surface. Consequently, an HRP-mediated conversion (10 min) of 4-CN to benzo-4-chlorocyclohexadienone with $H_2O_2$ yielded an insoluble precipitate on the sensor surface in which the biocatalyzed reaction took place.[29,30]

**2.3. Surface Plasmon Resonance Imaging System.** To obtain multichannel images of SAMs and protein interactions, we constructed a 2D-SPR imaging system. Figure 4A shows a schematic view of the SPR imaging system, and Figure 4B shows our constructed imaging system. A 100 W quartz tungsten−halogen (QTH) lamp was used as a light source in combination with a narrow band-pass filter ($\lambda_0$ = 633 nm, $\Delta\lambda$ = 1 nm). To couple light to the surface plasmon, a sheet polarizer was located in front of the prism coupler. Two objective lenses (L1 and L2) were used for the beam collimation and expansion, and a monochromatic light impinged on a prism coupler with a diameter of ~7 mm. A gold-coated sensor chip, on which SAMs or proteins were patterned, was optically coupled with a prism coupler via an index matching oil ($n_D$ = 1.517) and placed on the center of a goniometer (model 414, Huber Diffraktionstechnik). The goniometer was controlled electronically by a stepping motor controller. At the incident angle where the contrast was at a maximum, the reflected image was taken by a conventional $^1/_3$ in. charge-coupled device (CCD) camera (BCE-242LA, Kukjae), while monitoring the contrast images with an analogue monitor simultaneously. A plano-convex lens (L3) with a focal length of ~50 mm was placed in front of the bare CCD chip for sharper imaging. The images were then stored digitally in a personal computer by an 8-bit B/W frame grabber.

**2.4. Ellipsometry.** For the ellipsometry, freshly evaporated gold-coated chip surfaces were prepared by an electron beam evaporator. The 11-mercaptoundecanoic acid-SAM-modified gold surfaces were prepared by using the same procedure as that described above. Ellipsometric thicknesses were determined on a spectroscopic ellipsometer (model Uvisel, Jobin Yvon) with dried chips in air with a 70° angle of incidence at a 632.8 nm wavelength. At least five different locations on each sample were measured, and the average was calculated. Those ellipsometric thicknesses had an uncertainty level of ~2 Å.

## 3. Results and Discussion

Absorption of light by SPR can be represented as a function of incident angle or wavelength. In case of 2D-SPR, because the reflected image is represented by the difference of SP resonance condition at each point on the surface under fixed angle and wavelength, there is always a set of optimal angle and wavelength at which the maximal contrast can be obtained. In this study, we discuss the results which were obtained by the 2D-SPR imaging system for patterned chemical monolayers (SAMs) and for the biospecific interaction of proteins (IFN-$\gamma$ as a model analyte).

Figure 5A shows a 2D-SPR image obtained from the micropatterned chip surface at the maximum difference in contrast between the 11-mercaptoundecanoic acid SAM and the bare gold surface, where the incident angle of light is at $\theta_0$ = 44.2°. As was described in the Experimental Section, we employed a direct photooxidation of alkanethiols to alkanesufonates by UV light for the micropatterning. From the process, the 11-mercaptoundecanoic acid SAM in the exposed area of the microarray (diameter 300 $\mu$m holes) was photooxidized and removed by ethanol washing, so that the base gold surface was exposed, whereas the surrounding area was covered by an intact SAM. Although the original patterns of the array were in circular form, the shape was distorted in an oval shape from the refraction of reflected light. The contrast and resolution of the 2D-SPR images for a micropatterned 11-mercaptoundecanoic acid SAM was found to be sufficient for the analysis of molecular monolayer level of a few nanometer thickness. Depicted in Figure 5B is the line profile of two circular patterns of array, taken across the line in Figure 5A. Ordinate in the figure is the pixel value, averaged out from 20 pixels longitudinally, as a function of pixel points on the sensor surface. In addition, imaging results from the micropatterned 11-mercaptoundecanol SAM were essentially similar, but the optimal conditions of exposure time and light intensity for the photooxidation reaction were different (data not shown).

To investigate the thickness resolution of the 2D-SPR imaging in more detail, a comparative study with ellipsometry was performed. The ellipsometric measurement for the 11-mercaptoundecanoic acid SAM showed that the thickness of the SAM on the gold surface could be

(29) Patolsky, F.; Zayats, M.; Katz, E.; Willner, I. *Anal. Chem.* **1999**, *71*, 3171−3180.
(30) Yoon, H. C.; Yang, H.; Kim, Y. T. *Analyst* **2002**, *127*, 1082−1087.

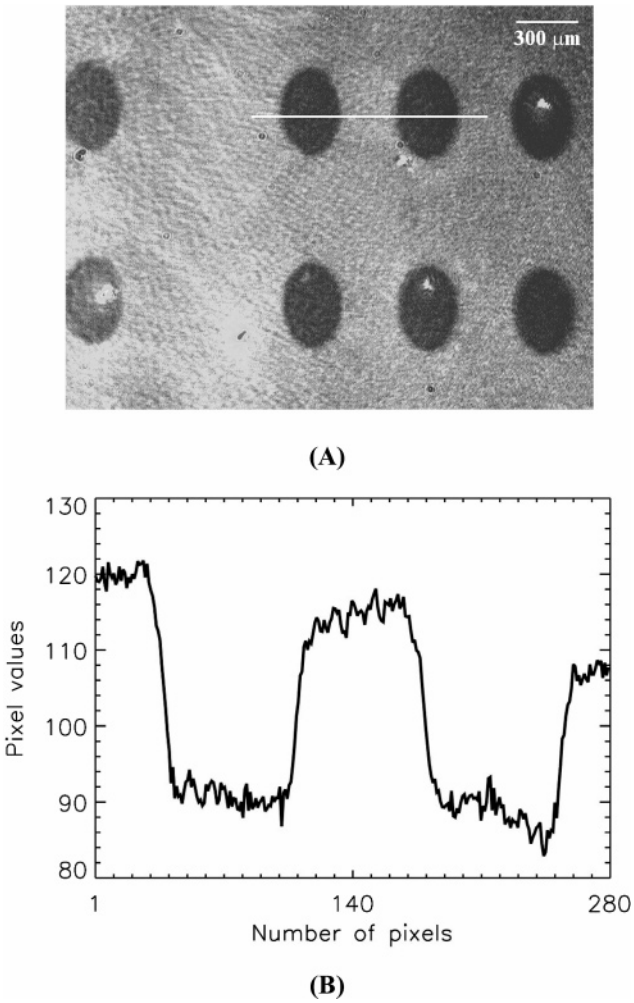


**Figure 5.** (A) 2D-SPR image of a micropatterned 11-mercaptoundecanoic acid SAM. Circular channels of 300 $\mu$m in diameter are exposed gold surface, whereas an intact SAM covers the surroundings. The collected images of channels are distorted by the refraction of reflected light. (B) A line profile of two array sites, taken across the line in part A. The pixel value represents the relative thickness variation on the surface.

estimated to be 1.6−1.9 nm, calculated from a refractive index of $n_{He-Ne} = 1.45$ based on those of hydrocarbons and mercaptans.[31,32] Here, we took the nominal value of the thickness of the 11-mercaptoundecanoic acid SAM to be 1.75 nm under the assumption that the SAM layer is close packed and slanted ~30° from normal. By comparing experimentally measured thicknesses of 11-mercaptoundecanoic acid monolayers and the contrast in the image in Figure 5B, we could estimate the thickness resolution of the 2D-SPR imaging system. With the n-phase Fresnel equation, the relationship between the thickness change of SAMs and the reflectivity of light for adsorbed SAMs on gold was calculated. From the calculation, it was found that, for a fixed incident angle of 44.5°, the reflectivity of incident light is linearly proportional to the thickness of the SAM when the thickness change is small, that is, up to a few nanometers (see the Supporting Information). From the ellipsometric study, we estimated the thickness of the 11-mercaptoundecanoic acid-SAM layer to be 1.75 nm, which corresponds to a reflectivity change of 21.09%. Since CCD responses with respect to incident light are

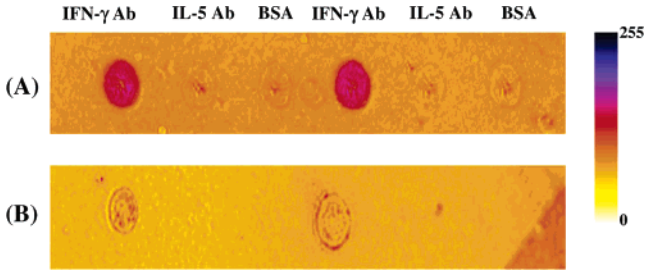


**Figure 6.** Detection of biospecific antigen/antibody interaction for IFN-$\gamma$ using the 2D-SPR imaging system with the signal enhancement by the peroxidase (HRP)-catalyzed precipitation reaction. Target protein (IFN-$\gamma$) concentrations: (A) 100 and (B) 1 ng/mL. The spotted proteins on the linear array are anti-IFN-$\gamma$ antibody, anti-IL-5 antibody, and BSA.

linear and we took the output look-up table (LUT) to be unity for digitization, an important relationship is thickness change versus reflectivity of light. From the line profile of registered 2D-SPR images in Figure 5B, the thickness of the 11-mercaptoundecanoic acid-SAM layer was about 30 ± 2 pixel values, which corresponds to a thickness of 1.75 ± 0.07 nm. With this result, we estimated that 2D-SPR could resolve the thickness difference with ~0.2 nm scale (3-fold of noise level), enabling the distinction of partially broken monolayers and the analysis of mixed SAMs.[33,34]

As an extension of the 2D-SPR imaging technology to the biochip analysis, we also investigated a biospecific recognition of antigen/antibody with the 2D-SPR imaging. Using a sandwich immunoassay of IFN-$\gamma$ antigen/anti-IFN-$\gamma$ antibody in combination with a precipitation scheme induced by a biocatalytic reaction, an array-type immunoanalysis was conducted (see Figure 3). For the immunoassay, the 11-mercaptoundecanol SAM on the gold surface was activated via NHS/EDA reaction. Capture antibodies, anti-IFN-$\gamma$ antibody, and anti-IL-5 antibody together with BSA as a control channel were regularly spotted (diameter 300 $\mu$m) by a microarrayer on the NHS-activated surface (Figure 6). At this stage, we could observe an image contrast resulting from the immobilization of proteins to the spotted area. However, the image contrasts were different from spot to spot, since the functionalization efficiency was dependent on the nature of applied proteins. To remove these false positive signals, a BSA back-filling step was added to cover the entire chip surface uniformly. After the reaction, a control 2D-SPR image was achieved, resulting in a uniform image with identical thickness data between spotted arrays and BSA-coated background areas (in orange color, Figure 6).

The sensor surface was then reacted with the target analyte, IFN-$\gamma$, of predetermined concentration and thoroughly washed with a buffer solution to remove nonspecifically bound IFN-$\gamma$. Next, the biotinylated detection antibody of IFN-$\gamma$ and enzyme-labeled avidin (avidin−HRP) was reacted successively. After the reaction, the resulting 2D-SPR chip surface having avidin−HRP/biotinylated anti-IFN-$\gamma$/IFN-$\gamma$ antigen/anti-IFN-$\gamma$ capture antibody/SAM association laminate was subjected to the signal generation/imaging step.

The biocatalyzed reaction of labeled peroxidase at the IFN-$\gamma$ positive arrays produced an insoluble precipitate that increased the thickness of the chip surface. The 2D-SPR reflection images of the chip surface were presented in Figure 6. In Figure 6A, a sample containing 100 ng/mL

(31) Bain, C. D.; Troughton, E. B.; Tao, Y. T.; Evall, J.; Whitesides, G. M.; Nuzzo, R. G. *J. Am. Chem. Soc.* **1989**, *111*, 321−335.
(32) West, R. C. *Handbook of Chemistry and Physics*; CRC Press: Boca Raton, FL, 1984.
(33) Ostuni, E.; Grzybowski, B. A.; Mrksich, M.; Roberts, C. S.; Whitesides, G. M. *Langmuir* **2003**, *19*, 1861−1872.
(34) Brewer, N. J.; Leggett, G. J. *Langmuir* **2004**, *20*, 4109−4115.

IFN-$\gamma$ with 1 mg/mL BSA was reacted with the protein arrays composed of anti-IFN-$\gamma$ antibody, anti-IL-5 antibody, and BSA to determine the immunosensing capability and the possibility of undesired cross-reactivity. The thickness change on the chip surface was scaled in pixel values ranging from 0 to 255. The biospecific binding of IFN-$\gamma$ antigen and anti-IFN-$\gamma$ antibody was distinctively shown as red spots. Other channels in the array, anti-IL-5 antibody, and BSA were essentially invisible, showing that the cross-reactivity was not significant. Still, when we reduced the sample concentration down to 1 ng/mL, as shown in Figure 6B, we could recognize the specific binding of IFN-$\gamma$ antigen and anti-IFN-$\gamma$ antibody, although the signal was not sufficient for a quantitative analysis.

In summary, we developed a 2D-SPR imaging system and obtained multichannel images of micropatterned SAMs and biospecific interactions at protein microarrays. From the calibration result of the 2D-SPR imaging system with the ellipsometric experimental data, a thickness sensitivity within a sub-nanometer level could be estimated. In addition, to evaluate the possibility of using the 2D-SPR system as an analytical platform for the protein chip, we also examined the biospecific interaction of antigen and antibody. From our investigations, the biospecific binding of IFN-$\gamma$ antigen with surface-immobilized antibody was found detectable down to a concentration of 1 ng/mL antigen employing a biocatalyzed amplification reaction. The optimized sensing condition, fulfilling the requirement of label-free immunoanalysis with desired sensitivity, is yet to be improved. Efforts to increase the sensitivity in the biorecognition reaction, including biochip surface design and protein engineering for capture antibody improvement, are currently underway.

**Acknowledgment.** Financial support by the Ministry of Information and Communication Korea (Grant Nos. 01MB2220 and 03MB2420) and the Korea Science and Engineering Foundation (Grant No. R05-04-10209) is gratefully acknowledged. Authors are also grateful to Dr. J. Ju (ETRI) for measuring optical data of the photoresist AZ5214E.

**Supporting Information Available:** Figures showing the proportionality of the reflectivity of light to the thickness of the adsorbed layer. This material is available free of charge via the Internet at http://pubs.acs.org.

LA0486382